JOC The Journal of Organic Chemistry

pubs.acs.org/joc Article

Gas-Phase Reactivity of Quinoline-Based Singlet Oxenium Cations

Xin Ma,[#] Ruth O. Anyaeche,[#] Erlu Feng, Erynn Johnson, Ethan Roller, Daniel J. Rumley, John J. Nash, and Hilkka I. Kenttämaa*

Cite This: J. Org. Chem. 2024, 89, 5458−5468 Read Online

ACCESS | Metrics & More | Article Recommendations | Supporting Information

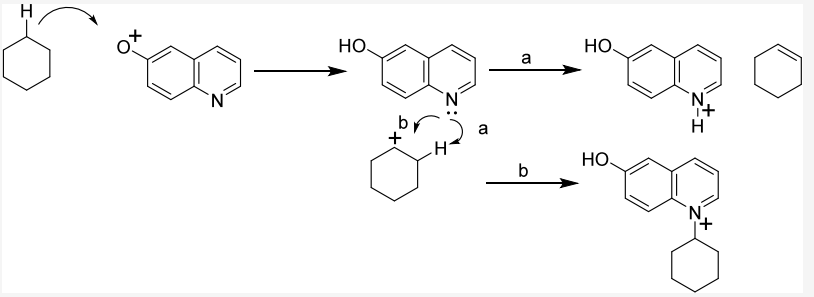

ABSTRACT: Isomeric quinolyloxenium cations were generated in the gas phase in an ion trap mass spectrometer to explore their reactions. The structures of some products were identified via collision-activated dissociation experiments involving model compounds to demonstrate that they have the expected heavy atom connectivity. The lack of radical reactions suggests that the cations have closed-shell singlet electronic ground states. Calculations (CASPT2/CASSCF(16,14)/cc-pVTZ//CASSCF(16,14)/cc-pVTZ) predict that their closed-shell singlet (^{1}A') ground states are lower in energy by ca. 25 kcal mol^{-1} than their lowest-lying excited states. All cations are reactive toward dimethyl disulfide, dimethyl sulfide, and allyl iodide and most toward water and moderately reactive toward cyclohexane, reflecting their strongly electrophilic nature. They form adducts with nucleophiles in exothermic reactions (ca. 50 kcal mol^{-1} for dimethyl sulfide) that can fragment or be stabilized via IR emission. Most water adducts spontaneously isomerize to lower-energy tautomers. The nucleophiles preferentially add to those carbon atoms in the benzene ring that have the greatest positive charge (but not the carbonyl carbon). The cations react with cyclohexane via hydride abstraction by the oxygen atom. This is the only reaction that initially involves the oxygen atom and hence reflects the formally positively charged, monovalent oxygen atom in these cations.

INTRODUCTION

Aryloxenium cations contain a formally positively charged, monovalent oxygen atom with an incomplete electron shell (Chart 1). They are key intermediates in the electrochemical and chemical oxidation of phenols.[1−3] They also have been implicated in astrochemical studies and are thought to persist in interstellar space.[4−7] The first detected aryloxenium cation was generated in aqueous solution via laser flash photolysis.[8,9] The parent phenyloxenium cation (Chart 1), also generated by laser flash photolysis, was identified via product analysis and trapping experiments.[10−13] The closed-shell singlet ground-state electronic configuration (calculated $\Delta E_{S\text{-}T}$: ca. −15 kcal mol^{-1}) for oxenium cations results from the strong interactions of the π system of the benzene ring with the out-of-plane p orbital of the oxygen atom, which breaks the frontier orbital degeneracy. With widely separated frontier orbitals, the closed-shell singlet state becomes the lowest-energy electron configuration.[14,15]

Chart 1. Phenyloxenium Cation with Several Resonance Structures

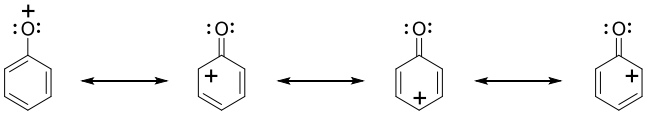

Unfortunately, neutral radical impurities have hampered the examination of the reactivity of phenyloxenium cations in a previous study.[16] Furthermore, these photolysis studies are limited by the lack of general (photo)precursors for the oxenium cations as well as their extremely short lifetimes (less than 1 μs) in solution.[14] As a result, most studies have focused on the mechanisms of generation of oxenium cations rather than on their chemical properties although a few products formed upon reactions with the solvent have been

Received: December 18, 2023
Revised: March 10, 2024
Accepted: March 19, 2024
Published: March 30, 2024

https://doi.org/10.1021/acs.joc.3c02895
J. Org. Chem. 2024, 89, 5458−5468

reported.[12,14] Thus, although aryloxenium ions have been investigated for more than 40 years,[17−20] studies concerning their reactivity lag far behind carbenium ions.

Here, the gas-phase reactivity of several quinolyloxenium cations (Chart 2) was examined by using linear quadrupole ion

Chart 2. Quinolyloxenium Cations 1−4

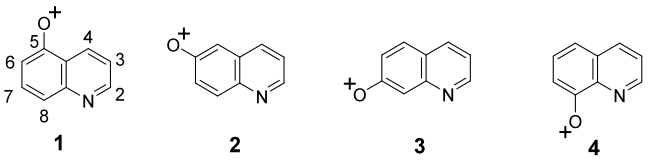

trap mass spectrometry. This study is not hampered by the formation of neutral radical impurities, as neutral reaction products are pumped out of the ion trap before examination of the reactions of the oxenium cations. Further, the reactions of the oxenium cations can be studied with a variety of reagents (and not just solvents), and the reaction kinetics can be explored. The experimental studies were complemented by high-level quantum chemical calculations.

METHODS

A Thermo LTQ linear quadrupole ion trap (LQIT) mass spectrometer was used to conduct all gas-phase experiments. The radical cations were generated using atmospheric-pressure chemical ionization (APCI) with CS_2 as the ionization reagent and solvent[21] and then transferred into the ion trap and isolated by ejecting all unwanted ions from the trap. Collision-activated dissociation (CAD; MS^2 experiments) was used to cleave a methyl or a nitrogen monoxide radical from the methoxy- or nitroquinoline radical cations, respectively (collision energy = 40, arbitrary units). The fragment ions were isolated and allowed to undergo reactions with a reagent in the ion trap (MS^3 experiments) for varying reaction times. Reagents were introduced into the ion trap via a reagent mixing manifold.[22−25] The data analysis has been discussed previously.[25,26]

RESULTS AND DISCUSSION

Generation of the Oxenium Cations. Initially, CAD experiments were performed on radical cations of methoxypyridines in an attempt to generate aryloxenium cations via the elimination of a methyl radical; however, only small amounts of ions possibly corresponding to the desired oxenium cations were detected. Subsequently, CAD of quinoline radical cations with a methoxy group on the pyridine ring was examined, but this approach also failed to generate large amounts of the desired oxenium cations. However, CAD of radical cations of quinolines with either a methoxy or nitro group in the benzene moiety (Chart 3) resulted in the fast elimination of a methyl or nitric oxide radical, respectively, thus generating cations with the m/z ratio of the desired oxenium cations (**1**−**4**; for examples, see Scheme 1 and Figure 1). The structures of the ions were probed via their reactivity

Chart 3. Precursor Radical Cations Used to Generate Oxenium Cations 1−4. One Resonance Structure Shown for Each

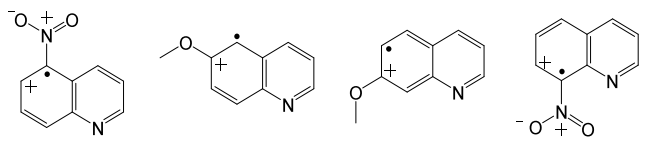

toward various reagents and via verification of the structures of some of their product ions via CAD experiments, as discussed below.[24,25,27,28]

Structural Elucidation of 1−4. The reagents dimethyl disulfide, allyl iodide, and cyclohexane (Table 1) were chosen to probe the structures of the ions thought to be **1**−**4** via ion−molecule reactions as these reagents are known to react with carbon-centered organic mono- and biradicals (but not even-electron cations) via transfer of one or two SCH_3 moieties, iodine atoms, or hydrogen atoms, respectively.[24,25,27,28] None of these radical reactions were detected for the cations expected to be **1**−**4**, as discussed below.

Upon reactions with dimethyl disulfide (Table 1 and Figure 2), abstraction of a SCH_3 moiety was not observed for the cations believed to correspond to **1**−**4**. Instead, a stable abundant adduct (m/z 238) was detected for **1**, **2**, and **3**. The adduct is not likely to be a secondary product generated upon consecutive abstraction of two SCH_3 moieties, which is common for organic biradicals,[27,28] since the abstraction of the first SCH_3 moiety was not detected. Instead, the adduct is likely a primary product generated upon the addition of the entire dimethyl disulfide to the cations.

Similarly to dimethyl disulfide, the most common radical reactions reported for allyl iodide (abstraction of one iodine atom from an allyl iodide molecule or consecutive abstraction of two iodine atoms from two allyl iodide molecules[25,27,28]) were not observed for the cations believed to be **1**−**4** (Table 1). Instead, abstraction of an allyl moiety was found to be the dominant reaction. This reaction has been previously reported for organic compounds not undergoing radical reactions, such as *ortho*-benzynes, and it involves nucleophilic addition of the carbon−carbon double bond of allyl iodide to the cation followed by a homolytic C−I bond cleavage.[25,27,28]

Upon reactions with cyclohexane, no single hydrogen atom abstraction products were detected for **1**−**4** (Table 1), in contrast to what has been reported for many carbon-centered radicals.[24,27,28] Instead, abundant product ions were formed that formally correspond to the addition of two hydrogen atoms to the oxenium cations. However, these product ions are likely formed upon an initial hydride anion abstraction followed by a proton abstraction (see discussion below), as previously reported for some aromatic even-electron cations.[24,27,28] Based on the above observations, it can be concluded that **1**−**4** do not contain unpaired electrons.

Further structural evidence is provided below, where the reactivities of **1**−**4** are discussed in detail. Most importantly, verification of the structures of some of their ionic reaction products via CAD in MS^4 experiments and comparison to the CAD behavior of ionized authentic model compounds was performed to verify the heavy atom connectivity of the oxenium cations. However, the results of quantum chemical calculations are discussed first.

Quantum Chemical Calculations for 1−4. The ground state for each of the oxenium cations **1**−**4** was calculated at the multiconfigurational self-consistent field (MCSCF) level of theory by using the correlation-consistent polarized valence-triple-ζ (cc-pVTZ[29]) basis set (the MCSCF calculations were of the complete active space (CASSCF) variety[30]). To improve the molecular orbital calculations for the ^{1}A', ^{1}A", ^{3}A', and ^{3}A" states of the quinolyloxenium cations **1**−**4**, dynamic electron correlation was also accounted for by using multireference second-order perturbation theory[31−33] (CASPT2) for multiconfigurational self-consistent field (MCSCF) reference wave

https://doi.org/10.1021/acs.joc.3c02895
J. Org. Chem. 2024, 89, 5458−5468

Scheme 1. Generation of Oxenium Cation 1 from the 5-Nitroquinoline Radical Cation (Top) and Oxenium Cation 2 from 6-Methoxy-quinoline Radical Cation (Bottom)

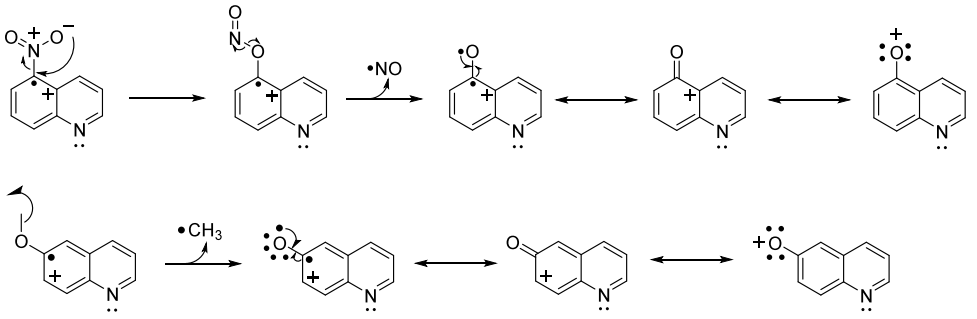

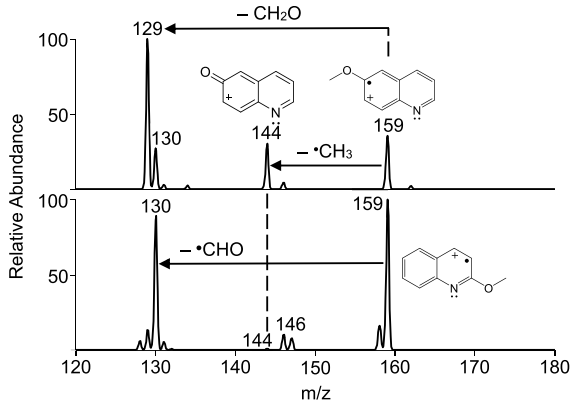

Figure 1. CAD mass spectra (MS^2 experiments) measured for the 6-methoxy- (top) and 2-methoxyquinoline radical cations (bottom). Note that only the radical cation with the methoxy group in the benzene ring (top) produces a relatively abundant fragment ion via the loss of a methyl moiety (m/z 144).

functions; these calculations were carried out for the CASSCF(16,14)/cc-pVTZ optimized geometries. All CASPT2/CASSCF and DFT calculations were carried out with the MOLCAS 8.0 and Gaussian 16 electronic structure program suites, respectively.[34,35] Each oxenium cation was calculated to be a closed-shell singlet (^{1}A') that lies ca. 22−27 kcal mol^{-1} lower in energy than the first excited state (i.e., ^{1}A" for **1** and **4** and ^{3}A' for **2** and **3**; calculated at the CASPT2/CASSCF(16,14)/cc-pVTZ//CASSCF(16,14)/cc-pVTZ level of theory; Table 2). The vertical electron affinities (EA_v) for the ground states of **1**−**4** and for the quinoline radical cation were also calculated (Table 2) to compare their electrophilicities. While the quinoline radical cation has the greatest calculated EA_v (8.46 eV), those of **1**−**4** are also high, with **3** having the largest (7.96 eV) and **4** having the smallest (7.73 eV) value. These findings suggest that **3** may be the most reactive and **4** the least reactive among the isomeric oxenium cations; however, the reactivity studies discussed below show that this is only the case for the water reagent (Table 1).

Atomic charges for the ground singlet states of **1**−**4** were also calculated (M06-2X/6-311++G(d,p)//CASSCF(16,14)/cc-pVTZ; CHELPG procedure;[36] Figure S1 in the SI). Based on these calculations, the carbon atom bearing the oxygen atom has the largest positive charge for **1**−**3**, whereas C-2 has the next largest positive charge. While nucleophilic addition reactions may not be expected to occur at the carbonyl carbon for any of these oxenium cations or at C-2 for two of them (**1** and **3**) (no stable singly charged product would be generated; this is supported by quantum chemical calculations described below), addition may occur at a few other sites based on the most reasonable resonance structures capable of forming a stable product upon addition (for example, see Chart 4 for **1** and Figure S2 for **2**−**4**).

In order to attempt to identify the most likely sites for nucleophilic addition, the reaction enthalpies for the addition of the hydride anion to **1**−**4** at several different sites were calculated (at the M06-2X/6-311++G(d,p)//M06-2X/6-311++G(d,p) level of theory). The reaction enthalpies calculated for the addition of the hydride anion in **1** to C-2, C-3, C-4, C-5 (carbonyl carbon), C-6, C-8, and O are −187.8 (a zwitterionic product is generated), −227.4, −188.9 (zwitterionic product), −225.3, −250.7, −251.8, and −260.3 kcal mol^{-1}, respectively. As expected, hydride addition is calculated to be most exothermic at the oxygen atom; however, the second and third most favorable addition sites are C-8 and C-6, with C-8 having just a slightly greater exothermicity. Indeed, C-8 is the second most and C-6 is the third most positively charged carbon atom (calculated atomic charges of +0.140 and −0.062, respectively; Figure S1 in the SI) in the benzene ring among those carbons that can form a stable, nonzwitterionic adduct (Chart 4 and Figure S1).

Overall, solely based on the exothermicities calculated for **1**, the hydride anion preferentially adds to atoms in the benzene ring and not the pyridine ring. In the benzene ring, the carbon atoms (C-8 and C-6) with the largest positive (least negative) charge that in principle can form a stable adduct are favored (after the oxygen atom).

The most favored hydride anion addition sites for **2** and **3**, after the oxygen atom, were calculated to be C-5 (−255.2 kcal mol^{-1}) and C-8 (−259.8 kcal mol^{-1}), respectively. Again, these addition sites correspond to the carbon atom in the benzene ring with the largest positive (least negative) charge (−0.039 and −0.118, respectively; with the exception of the carbonyl carbon). For **4**, hydride anion addition to C-5 and C-7 was calculated to be equally exothermic (−246.8 kcal mol^{-1}). Again, these two sites were calculated to carry the largest positive atomic charges in the benzene ring among the atoms that can, in principle, form a stable adduct (+0.186 and −0.008, respectively). Unfortunately, hydride anion addition reactions cannot be experimentally studied using the approaches employed here, as the product would be a neutral compound not detectable by mass spectrometry.

In order to further explore the identities of the most likely sites for nucleophilic addition to **1**−**4**, another reagent that can be experimentally studied, dimethyl sulfide, was examined. Dimethyl sulfide reacts to predominantly generate a stable addition product for **1**−**4** (Figure S3), with **4** producing the

https://doi.org/10.1021/acs.joc.3c02895
J. Org. Chem. 2024, 89, 5458−5468

Table 1. Reactions, Total Reaction Efficiencies,[a] and Branching Ratios for Ionic Primary Products for 1−4[b] upon Reactions with Dimethyl Disulfide, Allyl Iodide, Cyclohexane, and Water

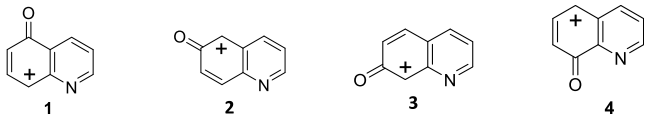

	1		2		3		4	
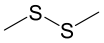	Addition	68%	Addition	57%	Addition	61%	CH_2 abs	44%
	e⁻ abs[c]	25%	e⁻ abs	21%	$H_2C{=}S$ abs	13%	CH_3 abs	31%
	CH_2 abs	5%	$HSCH_3$ abs	17%	CH_2 abs	11%	$H_2C{=}S$ abs	14%
	$H_2C{=}S$ abs	2%	$H_2C{=}S$ abs	5%	$HSCH_3$ abs	9%	e⁻ abs	4%
					e⁻ abs	6%	2° SCH_3 abs[d]	
							H^- abs	4%
							$HSCH_3$ abs	3%
	Efficiency	39%	Efficiency	69%	Efficiency	31%	Efficiency	81%
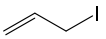	Allyl abs	73%	Allyl abs	98%	Allyl abs	97%	Allyl abs	100%
	Addition	27%	Addition	2%	Addition	3%		
	Efficiency	38%	Efficiency	60%	Efficiency	26%	Efficiency	55%
	2×H abs	78%	2×H abs	92%	2×H abs	91%	2×H abs	92%
	Addition	21%	Addition	7%	Addition	8%	Addition	6%
	H^- abs	1%	H^- abs	1%	H^- abs	1%	H^- abs	1%
							C_2H_4 abs	1%
	Efficiency	2%	Efficiency	20%	Efficiency	1%	Efficiency	13%
H_2O	Addition	100%	Addition	100%	Addition	100%	Addition	100%
	Efficiency	78%	Efficiency	22%	Efficiency	100%	Efficiency	1%

[a]A fast reaction with adventitious water competes with the reactions of **1−3** with all the desired reagents, which likely influences their reaction efficiencies to some extent. [b]For the selection of the specific resonance structures shown, see discussion below. [c]abs = abstraction. [d]2° indicates a secondary production of the primary production shown above.

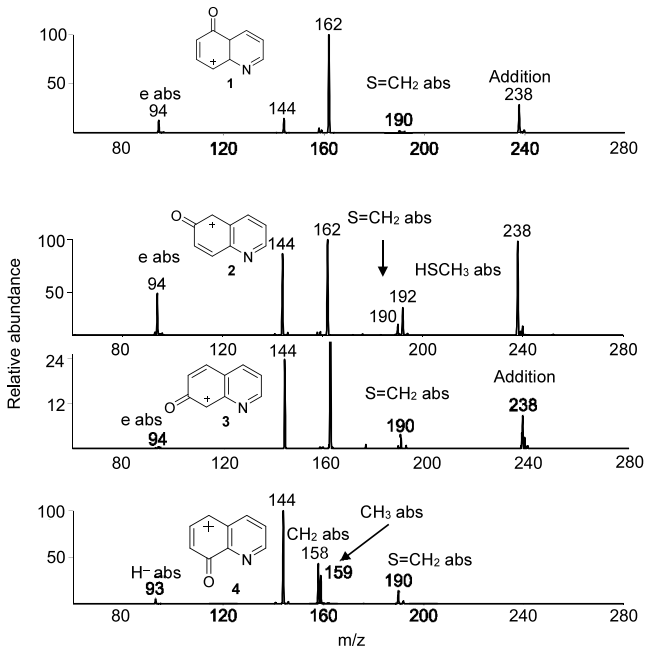

Figure 2. Mass spectra measured after 100 ms reactions of **1−4** (m/z 144) with dimethyl disulfide. Note that the ion of m/z 162 is a water adduct formed upon reactions of **1−3** with adventitious water in the ion trap.

Table 2. Calculated[a] Relative Enthalpies (H_{rel}, kcal mol^{-1}) for Ground and Excited States of 1−4, Calculated[b] Vertical Electron Affinities (EA_v, eV) for Ground States of 1−4, and Calculated[c] Vertical Electron Affinity of the Quinoline Radical Cation

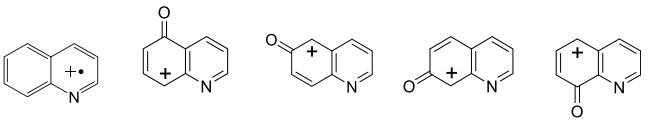

π-radical	1	2	3	4
H_{rel} (^{1}A' state)		0.0	0.0	0.0	0.0
H_{rel} (^{1}A" state)		26.9	28.7	28.5	24.8
H_{rel} (^{3}A' state)		32.1	25.9	22.3	34.9
H_{rel} (^{3}A" state)		27.2	28.0	24.8	26.4
EA_v (^{2}A" → ^{1}A')	8.46				
EA_v (^{1}A' → ^{2}A")		7.89	7.88	7.96	7.73

[a]Calculated at the CASPT2/CASSCF(16,14)/cc-pVTZ//CASSCF(16,14)/cc-pVTZ level of theory; corrected for zero-point vibrational energies and 298 K thermal energies by using the (unscaled) CASSCF(16,14)/cc-pVTZ frequencies. [b]Calculated at the CASPT2/CASSCF(17,14)/cc-pVTZ//CASSCF(16,14)/cc-pVTZ level of theory. [c]Calculated at the CASPT2/CASSCF(12,11)/cc-pVTZ//CASSCF(11,11)/cc-pVTZ level of theory.

adduct at the lowest efficiency, favoring hydride abstraction to generate $CH_3S{=}CH_2^+$ (m/z 61). Hydride abstraction was also detected for **1−3** although it was most abundant for **4** (Figure

https://doi.org/10.1021/acs.joc.3c02895
J. Org. Chem. 2024, 89, 5458−5468

Chart 4. Most Relevant Resonance Structures for 1. They Are, in Principle, Able to Generate a Stable Singly Charged Addition Product with a Neutral Nucleophile without Rearrangement. The Magnitudes of the Calculated Atomic Charges at the Different Sites Are C-8 > C-6 > C-3 > O (Figure S1)

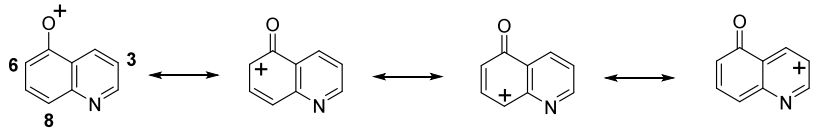

Chart 5. Most Relevant Resonance Structures for 1−4

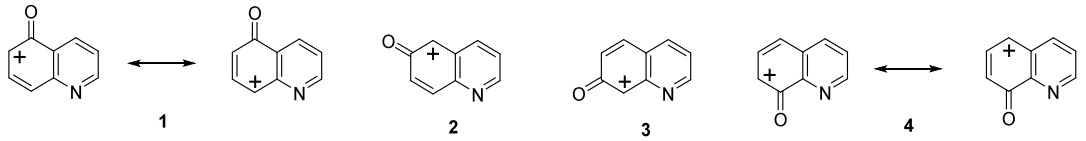

Scheme 2. Enthalpy Changes Calculated at the M06-2X/6-311G++G(d,p)//M06-2X/6-311G++(d,p) Level of Theory for Water Addition to 1 at Two Different Sites

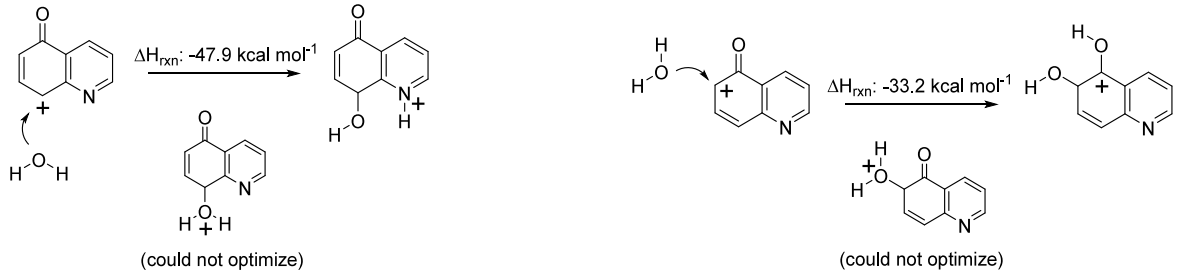

S3). Abstraction of both a hydride anion and a proton (via an unknown mechanism; m/z 146) was additionally detected.

The reaction enthalpies for the formation of an adduct with dimethyl sulfide at seven carbon atoms (C-2−C-8) in **1**−**4** were calculated (at the M06-2X/6-311++G(d,p)//M06-2X/6-311++G(d,p) level of theory; see the SI). Based on the calculated values, the favored addition sites for **2** (C-5) and **3** (C-8) are in agreement with the favored (carbon-centered) addition sites discussed above for the hydride anion (values for **2**: C-2, −27.0; C-4, −22.4; C-5, −50.3; C-7, −28.1; C-8, −26.3 kcal mol^{-1} (this rearranged structure contains a cyclopropanone ring); values for **3**: C-3, −27.1; C-4, −12.7 (rearranged to a cyclopropyl ring); C-5, −23.7 (rearranged to a cyclopropanone ring); C-6, −30.4; C-8, −59.4 kcal mol^{-1}). Addition products for **1** were found for addition of dimethyl sulfide to C-3, C-6, C-7 (rearranged a cyclopropyl ring) and C-8, with exothermicities of −19.6, −46.8, −35.5, and −46.6 kcal mol^{-1}, respectively. Therefore, the most and equally likely addition sites in **1** to produce a stable unrearranged addition product are C-6 and C-8. This finding is in agreement with the favored hydride anion addition sites discussed above. On the other hand, the results obtained for **4** are not in complete agreement with the hydride anion addition results. The most favored addition site for dimethyl sulfide was calculated to be C-7 with a reaction enthalpy of −44.9 kcal mol^{-1} followed by C-5, C-8 (rearranged structure has an epoxide ring), C-2, and C-4 (−39.4, −28.5, −23.5, and −13.7 kcal mol^{-1}, respectively), while C-5 and C-7 were calculated to be equally favorable for hydride anion addition. In conclusion, the most favorable sites for **1**−**4** to form an unrearranged stable adduct appear to be C-6 and C-8, C-5, C-8, and C-7 (or both C-5 and C-7), respectively, mostly reflecting the most positively charged (least negatively charged) carbon atom in the benzene ring (ignoring the carbonyl carbon).

It must be noted that the formation of a stable adduct under the experimental conditions used here almost certainly requires emission of IR light by the adduct[37] to release some of the excess energy that it is formed with so that insufficient energy remains to allow reverse dissociation to separated reactants or forward dissociation to fragmentation products (collisional cooling is not fast under the low-pressure conditions employed here).

Reactivities of 1−4. Based on the above considerations, the resonance structures shown for **1**−**4** in Chart 5 are used below to rationalize their reactivity. All of the oxenium cations **1**−**4** react with water only by formation of a stable addition product (Table 1). However, with one exception, these products undergo spontaneous rearrangement to generate substantially lower-energy adducts that have a longer lifetime and therefore are more likely to be stabilized by emission of light. For **1**, stable rearranged products were computationally found for addition of water at C-4, C-6, and C-8 (water addition computed for C-2 or C-3 did not produce a bound product), which have computed reaction enthalpies of −4.0, −33.2, and −47.9 kcal mol^{-1}, respectively (for some of these calculations, see Scheme 2). These computed enthalpies suggest that the thermodynamically most favorable addition site in **1** for water is C-8 (although addition to C-6 is also very favorable). However, the C-6 and C-8 sites were calculated to be equally favorable for the addition of both the hydride anion and dimethyl sulfide. Therefore, the specific energetically favorable rearrangement for the water adduct at C-8 makes this addition site more favorable than the C-6 site for water (Scheme 2).

For **2**, stable rearranged products were calculated for addition of water at C-5 and C-7 (only), having computed reaction enthalpies of −39.6 and −25.7 kcal mol^{-1}, respectively (Figure S2 in the SI). Hence, addition to C-5 is expected to

https://doi.org/10.1021/acs.joc.3c02895
J. Org. Chem. 2024, 89, 5458−5468

preferentially occur, and it yields the same structure as shown for **1** in Scheme 2 (right). This site was also calculated to be the most favorable addition site for the hydride anion and dimethyl sulfide molecule. For **3**, stable rearranged products were found for addition of water at C-6 and C-8 (only), having computed reaction enthalpies of −30.3 and −61.4 kcal mol^{-1}, respectively (Figure S2). Therefore, the reaction with water would be expected to occur preferentially at C-8, generating the rearranged structure shown in Chart 6. Again, this site is

Chart 6. Most Stable (Rearranged) Water Addition Product of 3

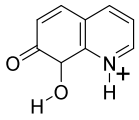

the favored addition site for the hydride anion and dimethyl sulfide molecule. For **4**, stable addition products were found computationally for the addition of water at C-7 and C-5 (only), which have computed reaction enthalpies of −31.9 and −6.1 kcal mol^{-1}, respectively (Figure S2). These addition sites are in agreement with those calculated for hydride and dimethyl sulfide addition (C-7 or both C-5 and C-7).

The lowest reactivity of **4** (reaction efficiency, 1%; Table 1) among **1**−**4** (reaction efficiencies for **1**−**3**: 78, 22, and 100%, respectively) is likely explained by its lowest addition/rearrangement reaction enthalpy (−31.9 kcal mol^{-1}; those of **1**−**3** are −47.9, −39.6, and −61.4 kcal mol^{-1}, respectively; Figure S2). It is interesting to note that only for **4**, a stable, unrearranged water adduct (at C-5) was calculated (Scheme 3). As the water adduct formed at C-5 is not adjacent to other substituents, it cannot readily rearrange.

Scheme 3. Addition of Water to 4 to the Two Most Likely Addition Sites C-5 (−6.1 kcal mol^{-1}) and C-7 (−31.3 kcal mol^{-1}) Having the Most Positive (Least Negative) Calculated Atomic Charge (Carbonyl Carbon Not Considered) in the Benzene Ring[a]

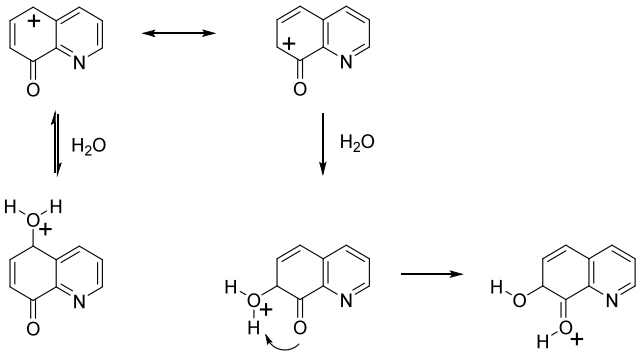

[a]The rearrangement reaction calculated to be the most exothermic (Figure S2) is shown.

In summary, the favored reaction sites for water in **2**, **3**, and **4** are concluded to be C-5, C-8, and C-7, respectively, while that for **1** (as discussed above) is C-8, closely followed by C-6. These sites are in agreement with the most important resonance structures shown in Chart 5. Upon addition of water, a highly exothermic rearrangement takes place for all of the water adducts, with the exception of that formed for **4** at C-5.

Collision-activated dissociation (CAD) experiments were performed to obtain information on the structures of the (isolated) rearranged water adducts of **1**−**3**. While the water adducts of **1** and **2** fragment via exclusive elimination of a water molecule, which is not structurally informative, that of **3** also eliminates carbon monoxide (Figure S5). This can be rationalized by the favored reaction site for **3** (C-8) being in close proximity to the basic nitrogen atom (which is not the case for **1** and **2**); hence, the adduct of **3** can rearrange while the carbonyl group remains intact (Scheme 4). Indeed, this specific rearrangement is calculated to be the most exothermic rearrangement for this water adduct of **3** (Figure S2 in the SI) and is calculated to be highly exothermic (−61.4 kcal mol^{-1}), which likely facilitates the elimination of carbon monoxide. The only other adduct that (based on calculations) contains an intact carbonyl group and hence could eliminate carbon monoxide is that of **1** after addition to C-8, but its rearrangement is substantially less exothermic than that for **3** (−47.9 kcal mol^{-1}). The difference of 13.5 kcal mol^{-1} in the reaction enthalpies for these two rearrangement reactions may explain why only the adduct of **3** eliminates carbon monoxide upon CAD.

Upon reactions of **1**−**4** with dimethyl disulfide, abundant stable unrearranged adduct ions (m/z 238) were detected for **1**−**3** but not for **4**, which is similar to the reactions of **1**−**4** with water (Table 1 and Figure 2). The reaction enthalpies for the addition of dimethyl disulfide at four different sites, O, C-2, C-7, and C-5, in **2** were calculated (M06-2X/6-311++G(d,p)//M06-2X/6-311++G(d,p)) to be −37.0, −27.6, −27.4, and −45.4 kcal mol^{-1}, respectively. Therefore, the favored addition site for **2** (C-5) is the same as that calculated for the hydride anion, dimethyl sulfide, and water additions (see above). The same is assumed to be the case for **1**, **3**, and **4**.

Calculated (M06-2X/6-311++G(d,p)//M06-2X/6-311++G(d,p)) reaction enthalpies for addition of dimethyl disulfide to C-8 in **1**, C-5 in **2**, and C-8 in **3** are −43.4, −45.4, and −54.4 kcal mol^{-1}, respectively. These addition reactions are highly exothermic, which explains why some of the adducts spontaneously fragment after formation. For example, elimination of $HSCH_3$ from the adduct of **3** (yielding the ion of m/z 190; Figure 2) has a transition state that lies 65.1 kcal mol^{-1} above the adduct of **3** (Figure 3; the structures were optimized at the density functional (DFT) level of theory by using the M06-2X functional[38] and the 6-311++G(d,p) basis set[39]). As the addition reaction is exothermic by 54.4 kcal mol^{-1}, only an additional 10.7 kcal mol^{-1} is needed to cause the fragmentation of the adduct.

The structures and the fragmentation behavior of the stable adduct ions detected for **1**−**3** were examined by isolating them and subjecting them to CAD. No fragment ions corresponding to the loss of a SCH_3 moiety (m/z 191) were detected in the CAD mass spectra measured for the adduct ions of m/z 238 formed from **1**−**3** (Figure 4), unlike for the dimethyl disulfide adducts of biradical cations that have been proposed[42] to be formed by consecutive addition of a thiomethyl moiety at each radical site. This finding, in particular, provides further support for the conclusion made above that the addition reaction with dimethyl disulfide is not a two-step radical reaction but instead a nucleophilic addition of the entire dimethyl disulfide molecule to the oxenium cations. Furthermore, the formation of an abundant dimethyl disulfide radical cation was observed

https://doi.org/10.1021/acs.joc.3c02895
J. Org. Chem. 2024, 89, 5458−5468

Scheme 4. Addition of Water to C-8 of 3 Followed by a Highly Exothermic Rearrangement[a]

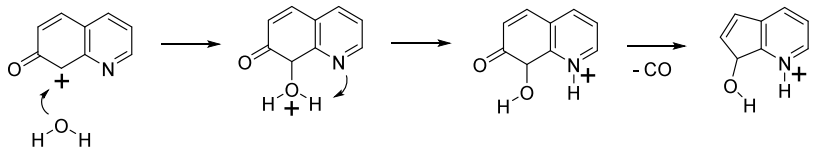

[a]ΔH (calc.): −61.4 kcal mol^{-1}. The excess energy gained in this rearrangement may facilitate more extensive dissociation than elimination of water, such as the loss of carbon monoxide, only detected for **3**.

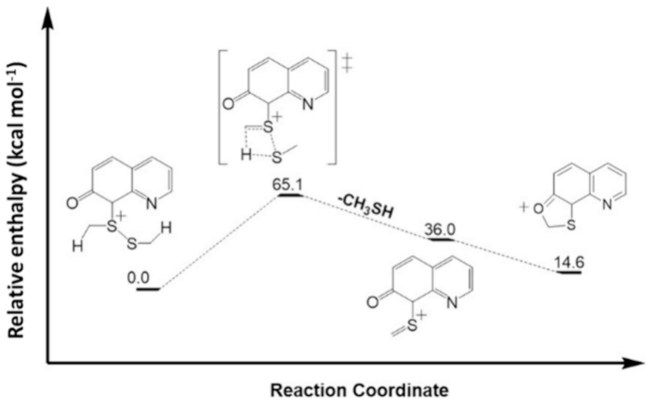

Figure 3. Calculated (M06-2X/6-311++G(d,p)//M06-2X/6-311++G(d,p)) relative enthalpies (kcal mol^{-1}) for the fragmentation of the dimethyl disulfide adduct of **3** via the elimination of CH_3SH (yielding a product ion of m/z 190).

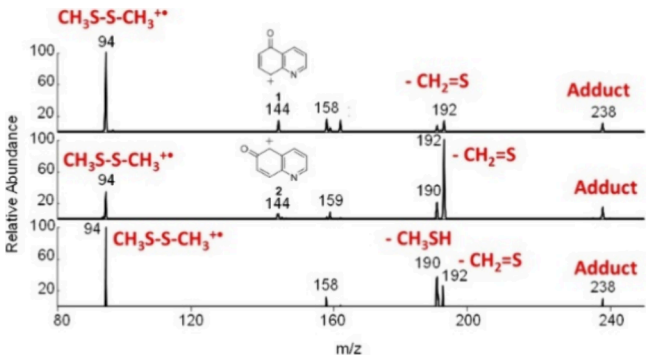

Figure 4. CAD mass spectra of the dimethyl disulfide adduct ions (m/z 238) of **1**−**3** (from top to bottom) (collision energy 15, arbitrary unit). The ions of m/z 158 likely involve the elimination of methyl disulfide (see discussion below), while those of m/z 159 likely involve the elimination of a methyl disulfide radical. The ion at m/z 162 in the top mass spectrum is a water adduct of the oxenium cation fragment (m/z 144). The ions of m/z 94 correspond to dimethyl disulfide radical cations.

upon CAD of all three adduct ions studied (Figure 4), which supports the assumption that the S−S bond of dimethyl disulfide remained intact upon adduct formation.

Further, CAD caused the elimination of CH_3SH via a rearrangement reaction from the adduct ions (formally corresponding to CH_2═S abstraction from dimethyl disulfide). Based on quantum chemical calculations, this reaction may occur, as shown in Figure 3 for **3**, to yield ions of m/z 190. Finally, elimination of CH_2═S (formally corresponding to CH_3SH abstraction from dimethyl disulfide) to generate fragment ions of m/z 192 also occurred upon CAD of the adducts (for quantum chemical calculations on the mechanism of this reaction for **2** and **3**, see Figure S6 in the SI). All of these findings suggest that the oxenium cations react with dimethyl disulfide via exothermic nucleophilic addition to generate unrearranged adducts, which occasionally undergo fragmentation involving rearrangement reactions.

Drastically different behavior was observed for **4**. No stable adduct was detected for this cation (Table 1). This observation is in agreement with the calculated reaction enthalpies for addition of dimethyl disulfide to **1**−**4** that is the lowest (only −38.5 kcal mol^{-1}) for **4** (at C-7; the values for the most favorable sites in **1**−**3** are −44.8, −45.4, and −54.4 kcal mol^{-1}, respectively). However, **4** can form a more stable adduct via a different mechanism, but this adduct is not kinetically stable, as discussed below.

An ion−molecule reaction product ion of m/z 158 formally corresponding to CH_2 abstraction from dimethyl disulfide was abundant only for **4** (Table 1). The potential energy surface calculated for this reaction (Figure 5) indicates that the reaction is initiated by an exothermic hydride transfer from dimethyl disulfide to the oxygen atom in **4**, which is in agreement with the results discussed above for the preference of the hydride anion to add to the oxygen atom in these oxenium cations. This initial reaction step is supported by the observation of the hydride abstraction product (although minor) for **4** but not for the other oxenium cations (ion of m/z 93, Table 1). The hydride abstraction transition state is the highest energy point in the potential energy surface (−20.9 kcal mol^{-1}; Figure 5), which explains why the abundance of the hydride abstraction product was very low: it undergoes fast exothermic reactions after formation to eventually generate the CH_2 abstraction product via the assistance of the pyridine nitrogen atom (Figure 5). The entire reaction sequence is calculated to be highly exothermic (by −56.5 kcal mol^{-1}; Figure 5) and involves the generation of a resonance-stabilized cyclized product.

In order to test the mechanism shown in Figure 5, reactions of **1**−**4** with dimethyl sulfide were also examined. Again, the analogous product formed via CH_2 abstraction was abundant only for **4** (Figure S3), which provides support to the mechanism proposed for dimethyl disulfide (Figure 5).

As mentioned above, the most common radical reaction reported for allyl iodide (I atom abstraction) was not observed for **1**−**4** (Figure S6 and Table 1).[27] Instead, abstraction of an allyl moiety via addition to the oxenium cations followed by the elimination of an iodine atom was the dominant reaction for **1**−**4** (with minor formation of a stable adduct; Table 1) and may occur as shown in Scheme 5 for **1**. This is not entirely surprising as this reaction has also been detected for *ortho*-benzyne analogs that have large singlet−triplet splittings and that do not undergo radical reactions.[28]

A stable adduct was also generated for **1**−**3** but not for **4** (Table 1). When this adduct was subjected to CAD, an iodine atom was eliminated to generate a product corresponding to the allyl moiety abstraction product (for **1**, see Figure S8). This

https://doi.org/10.1021/acs.joc.3c02895
J. Org. Chem. 2024, 89, 5458−5468

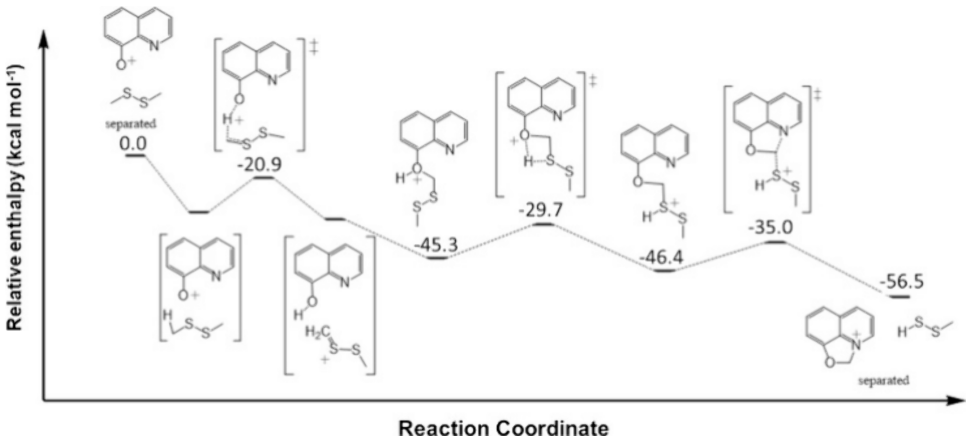

Figure 5. Calculated (M06-2X/6-311++G(d,p)//M06-2X/6-311++G(d,p)) relative enthalpies (kcal mol^{-1}) for CH_2 abstraction (product ion of m/z 158) from dimethyl disulfide by the 8-oxenium cation **4** (m/z 144) via formation of $CH_3{-}S{-}S^{+}{=}CH_2$ (m/z 93 in Figure 2) to yield a product ion of m/z 158. Note that the direct addition of dimethyl disulfide to C-5 in **4** is only exothermic by −35.4 kcal mol^{-1}; hence, the adduct shown above at −45.3 kcal mol^{-1} is lower in enthalpy, but it is unstable toward fragmentation.

Scheme 5. Mechanism Proposed for the Reaction of 1 with Allyl Iodide[a]

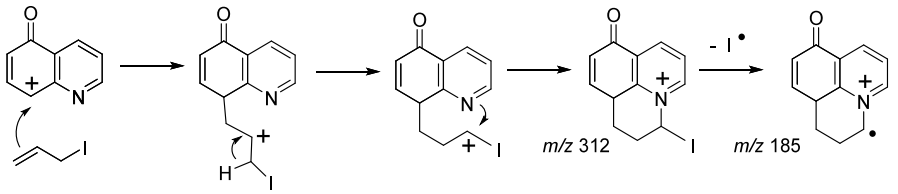

[a]Involving nucleophilic addition to one of the most favorable sites and stabilization of the adduct via the pyridine nitrogen atom to generate a resonance-stabilized adduct (m/z 312). In most instances, the adduct fragments by iodine atom elimination to generate the ion of m/z 185 corresponding to abstraction of an allyl moiety from allyl iodide.

finding indicates that the allyl abstraction products formed in the ion−molecule reactions are likely generated upon spontaneous fragmentation of the adducts of **1**−**4** due to the exothermicity of the addition reactions. Stabilization of some of the initially formed adducts may occur via the formation of a five-membered ring, as shown in Scheme 5 for **1**.

Finally, upon reactions of **1**−**4** with cyclohexane, no single hydrogen atom abstraction (ion of m/z 145) was observed (Figure 6 and Table 1). Instead, a reaction almost certainly involving a hydride abstraction followed by a proton abstraction occurred (to generate ions of m/z 146; for **1**, see Scheme 6, top), in agreement with a report for some aromatic even-electron cations.[28] This proposal is supported by the detection of a (minor) hydride abstraction product for **1**−**4** (Table 1). In order to further explore the site of hydride abstraction in the oxenium cations (i.e., beyond the calculations discussed above regarding the addition of the hydride anion), the sites of endothermic hydride abstraction from methane were calculated for **1**−**4** (Figures S8−S11). As expected, the lowest-energy hydride abstraction reaction involved the oxygen atom, and this reaction was at least 9 kcal mol^{-1} less endothermic than abstraction by the carbon atoms in the benzene ring. Based on these calculations, the same is assumed to be true for hydride abstraction from cyclohexane (although these hydride abstraction reactions are expected to be exothermic as they were detected; Table 1). It should be noted that hydride abstraction is the only reaction detected here that initially involves the oxygen atom and hence reflects the formally positively charged, monovalent oxygen atom in these cations.

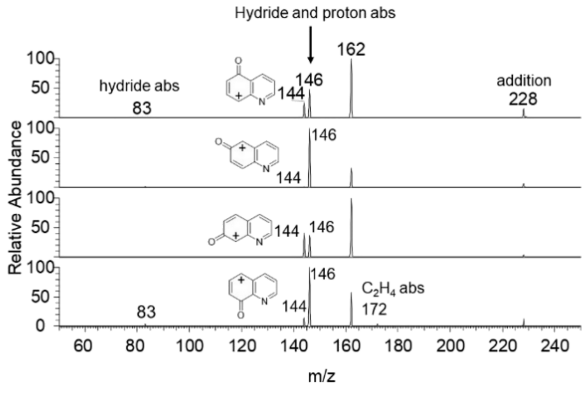

Figure 6. Mass spectra measured after 1000 ms reactions of **1**−**4** (m/z 144) with cyclohexane. The ion of m/z 162 is an adduct formed upon reactions of **1**−**4** with adventitious water in the ion trap. The ion of m/z 172 in the bottom mass spectrum is likely generated from the adduct (m/z 228) via the elimination of two ethylene molecules.

CAD was used to determine the structures of the hydride/proton abstraction product ions of m/z 146 generated from **2** and **4**. Both have the expected protonated hydroxyquinoline structure (6-hydroxy- and 8-hydroxyquinoline, respectively; see Scheme 6 for **2**) based on a comparison of their CAD fragmentation patterns to those of protonated authentic 6- and 8-hydroxyquinoline isomers (note that these two isomers fragment differently and can be differentiated from each other; Figures S13 and S14 in the SI). These findings confirm that the

https://doi.org/10.1021/acs.joc.3c02895
J. Org. Chem. 2024, 89, 5458−5468

Scheme 6. Likely Mechanisms (Pathway a) for the Formation of the Ion of *m*/*z* 146 (Top Right) from 2 via Hydride Abstraction Followed by Proton Abstraction from Cyclohexane and (Pathway b) for the Formation of the Stable Adduct of *m*/*z* 228 upon Reactions of 2 with Cyclohexane[a]

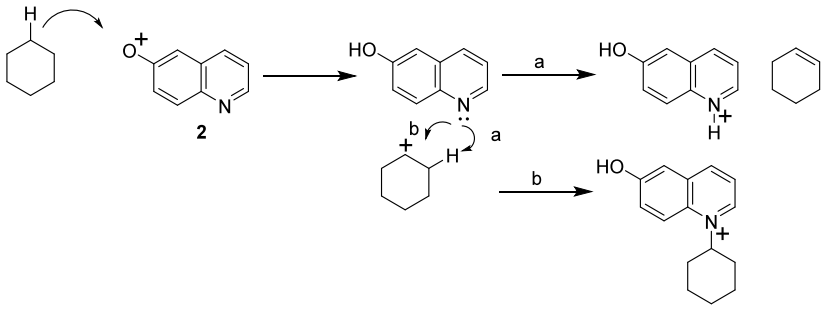

[a]Note that the cyclohexyl cation may rearrange to the 1-methylcyclopentyl cation during the reaction. The structure of the ion of *m*/*z* 146 (top right) was verified by CAD and comparison to an authentic compound (Figure S13).

oxenium cations **2** and **4** did not rearrange after formation and that they had the indicated heavy atom connectivity.

Finally, the relative reactivities of **1**−**4** toward the different reagents are considered. Formation of a stable adduct under the experimental conditions employed here is likely to be ultimately controlled by the rate of emission of IR light by the adduct[37] and hence does not reflect chemical reactivity. However, **4** does not rapidly form a stable adduct with most of the reagents discussed above; therefore, stabilization of the adduct via the emission of light does not need to be considered when comparing its reactivity toward those reagents. Thus, the relative reactivities of **4** toward the different reagents (with the exception of water) are expected to be fairly accurately represented by the reaction efficiencies in Table 1 (but those reported for **1**−**3** may not be). Based on this consideration, **4** is the most reactive toward allyl iodide (reaction efficiency, 100%), almost as reactive toward dimethyl disulfide (81%) and substantially less reactive toward cyclohexane (that is not a nucleophile; 13%). These relative reaction efficiencies are as expected for a strong electrophile (allyl iodide and dimethyl disulfide can be expected to be nearly equally nucleophilic based on their proton affinities; calculated[40] to be 193.4 kcal mol^{-1} and measured[41] to be 194.9 kcal mol^{-1}, respectively).

CONCLUSIONS

The quinolyloxenium cations generated in gas-phase experiments in a linear quadrupole ion trap mass spectrometer were demonstrated to have the expected heavy atom connectivity via the identification of some of their products generated upon abstraction of a hydride and a proton from cyclohexane via collision-activated dissociation (CAD) experiments and model compound studies. No diagnostic radical reactions (e.g., abstraction of a SCH_3 moiety from dimethyl disulfide, abstraction of an iodine atom from allyl iodide, or abstraction of a hydrogen atom from cyclohexane) were detected, in agreement with quantum chemical calculations that predict the closed-shell singlet ground states to be 22−29 kcal mol^{-1} lower in energy than their lowest-lying excited states. Instead, highly exothermic nonradical addition reactions (by 44.9−50.3 kcal mol^{-1} for dimethyl sulfide) were found to dominate, occasionally followed by fragmentation. Some of the adducts are likely stabilized by the emission of IR light because, under the experimental conditions employed here, collisional stabilization is not efficient.

Examination of CAD of several of the isolated adducts suggested that most of the adducts contain all of the atoms of the neutral reagent. However, some of the CAD behavior of the water adducts and calculations on the exothermicity of addition/rearrangement reactions for the water adducts support the hypothesis that most of these adducts spontaneously undergo highly exothermic isomerization reactions that provide them with a longer lifetime, which facilitates the stabilization of the adducts via emission of IR light. Furthermore, CAD experiments suggest that most products formed in the studied ion−molecule reactions arise from fragmentation of the adducts due to the exothermicity of the adduct formation.

For cyclohexane, hydride abstraction by the oxenium cations **1**−**4** was found to initiate the reactions. Based on calculations performed for reactions with the hydride anion and with methane, the oxygen atom of the cations is the most favorable site for hydride abstraction. This is the only reaction that initially involves the oxygen atom and hence reflects the formally positively charged, monovalent oxygen atom in these cations. All other reactions involve the carbon atoms of the oxenium cations.

Addition of reagents to each of the oxenium cations could potentially occur at several different sites. However, based on several pieces of evidence, it is concluded that addition predominantly occurs at the most positively (least negatively) charged carbon atom (based on calculated atomic charges) in the benzene ring (ignoring the carbonyl carbon) instead of the pyridine ring.

ASSOCIATED CONTENT

Data Availability Statement

The data underlying this study are available in the published article and its Supporting Information.

Supporting Information

The Supporting Information is available free of charge at https://pubs.acs.org/doi/10.1021/acs.joc.3c02895.

Experimental and computational details, calculated electrostatic charges in **1**−**4** and their relevant resonance structures, additional calculated potential energy surfaces, additional mass spectra and CAD mass spectra, second-order reaction rate constants measured for the ion−molecule reactions, synthesis of the radical precursor for **5**, and Cartesian coordinates for all calculations (PDF)

https://doi.org/10.1021/acs.joc.3c02895
J. Org. Chem. 2024, 89, 5458−5468

AUTHOR INFORMATION

Corresponding Author

Hilkka I. Kenttämaa − *Department of Chemistry, Purdue University, West Lafayette, Indiana 47906, United States;* orcid.org/0000-0001-8988-6984; Email: hilkka@purdue.edu

Authors

Xin Ma − *Department of Chemistry, Purdue University, West Lafayette, Indiana 47906, United States;* orcid.org/0000-0002-7058-0165

Ruth O. Anyaeche − *Department of Chemistry, Purdue University, West Lafayette, Indiana 47906, United States*

Erlu Feng − *Department of Chemistry, Purdue University, West Lafayette, Indiana 47906, United States*

Erynn Johnson − *Department of Chemistry, Purdue University, West Lafayette, Indiana 47906, United States*

Ethan Roller − *Department of Chemistry, Purdue University, West Lafayette, Indiana 47906, United States*

Daniel J. Rumley − *Department of Chemistry, Purdue University, West Lafayette, Indiana 47906, United States*

John J. Nash − *Department of Chemistry, Purdue University, West Lafayette, Indiana 47906, United States*

Complete contact information is available at: https://pubs.acs.org/10.1021/acs.joc.3c02895

Author Contributions

#X.M. and R.O.A. have made an equal contribution to this work.

Author Contributions

X.M. performed the initial experiments and initial manuscript writing; R.O.A. performed most of the experiments and some calculations and helped in manuscript writing; E.F. performed some calculations; E.J. helped with the experiments; E.R. performed the final experiments on dimethyl sulfide; D.J.R. performed the initial experiments on dimethyl sulfide; J.J.N. performed most of the calculations and finalization of the manuscript; H.K. performed supervision and finalization of the manuscript.

Notes

The authors declare no competing financial interest.

ACKNOWLEDGMENTS

The authors gratefully acknowledge the Purdue Research Foundation (PRF; grant number 60000025) for financial support. This material is also based upon work supported by the National Science Foundation under Grant No. 2154079.

REFERENCES

(1) Novak, M.; Glover, S. A. The Hydrolysis of 4-Acyloxy-4-substituted-2,5-cyclohexadienones: Limitations of Aryloxenium Ion Chemistry. *J. Am. Chem. Soc.* **2005**, *127*, 8090−8097.

(2) Rodrigues, J. A. R.; Abramovitch, R. A.; de Sousa, J. D. F.; Leiva, G. C. Diastereoselective Synthesis of Cularine Alkaloids via Enium Ions and an Easy Entry to Isoquinolines by Aza-Wittig Electrocyclic Ring Closure. *J. Org. Chem.* **2004**, *69*, 2920−2928.

(3) Pelter, A.; Ward, R. S. Two-electron Phenolic Oxidations Using Phenyliodonium Dicarboxylates. *Tetrahedron* **2001**, *57*, 273−282.

(4) Siuzdak, G.; North, S.; BelBruno, J. J. Multiphoton Ionization of Phenol in Nonaqueous Solutions: Characterization of the Cation and Ion−molecule Chemistry. *J. Phys. Chem.* **1991**, *95*, 5186−5190.

(5) Reiner, E. J.; Harrison, A. G. Energy Dependence of the Fragmentation of Haloanisole Molecular Ions. *Int. J. Mass Spectrom. Ion Processes* **1984**, *58*, 97−112.

(6) Leyva, E.; Platz, M. S.; Persy, G.; Wirz, J. Photochemistry of Phenyl Azide: the Role of Singlet and Triplet Phenylnitrene as Transient Intermediates. *J. Am. Chem. Soc.* **1986**, *108*, 3783−3790.

(7) Smith, D. The Ion Chemistry of Interstellar Clouds. *Chem. Rev.* **1992**, *92*, 1473−1485.

(8) Wang, Y.-T.; Wang, J.; Platz, M. S.; Novak, M. Direct Detection of a Transient Oxenium Ion in Water Generated by Laser Flash Photolysis. *J. Am. Chem. Soc.* **2007**, *129*, 14566−14567.

(9) Wang, Y.-T.; Jin, K. J.; Leopold, S. H.; Wang, J.; Peng, H.-L.; Platz, M. S.; Xue, J.; Phillips, D. L.; Glover, S. A.; Novak, M. Characterization of Reactive Intermediates Generated During Photolysis of 4-Acetoxy-4-aryl-2,5-cyclohexadienones: Oxenium Ions and Aryloxy Radicals. *J. Am. Chem. Soc.* **2008**, *130*, 16021−16030.

(10) Novak, M.; Poturalski, M. J.; Johnson, W. L.; Jones, M. P.; Wang, Y.; Glover, S. A. 4′-Substituted-4-biphenylyloxenium Ions: Reactivity and Selectivity in Aqueous Solution. *J. Org. Chem.* **2006**, *71*, 3778−3785.

(11) Wang, Y.-T.; Novak, M. Multiple Decomposition Pathways for the Oxenium Ion Precursor O-(4-(4′-Methylphenyl)phenyl)-N-methane-sulfonylhydroxylamine. *J. Org. Chem.* **2009**, *74*, 7697−7706.

(12) (a) Du, L.; Qiu, Y.; Lan, X.; Zhu, R.; Phillips, D. L.; Li, M.-D.; Dutton, A. S.; Winter, A. H. Direct Detection of the Open-Shell Singlet Phenyloxenium Ion: An Atom-Centered Diradical Reacts as an Electrophile. *J. Am. Chem. Soc.* **2017**, *139*, 15054−15059. (b) Qiu, Y.; Fischer, L. J.; Dutton, L. J.; Winter, A. H. Aryl Nitrenium and Oxenium Ions with Unusual High-Spin π,π^* Ground States: Exploiting (Anti)Aromaticity. *J. Org. Chem.* **2017**, *82*, 13550−13556.

(13) Soriente, A.; De Rosa, M.; La Manna, P.; Talotta, C.; Gaeta, C.; Spinella, A.; Neri, P. Exploiting the *p*-Bromodienone Route for the Formation and Trapping of Calixarene Oxenium Cations with Enamine Nucleophiles. *J. Org. Chem.* **2018**, *83*, 5947−5953.

(14) Hanway, P. J.; Xue, J.; Bhattacharjee, U.; Milot, M. J.; Ruixue, Z.; Phillips, D. L.; Winter, A. H. Direct Detection and Reactivity of the Short-Lived Phenyloxenium Ion. *J. Am. Chem. Soc.* **2013**, *135*, 9078−9082.

(15) Li, M.-D.; Hanway, P. J.; Albright, T. R.; Winter, A. H.; Phillips, D. L. Direct Spectroscopic Observation of Closed-Shell Singlet, Open-Shell Singlet, and Triplet *p*-Biphenylyloxenium Ion. *J. Am. Chem. Soc.* **2014**, *136*, 12364−12370.

(16) Qiu, Y.; Winter, A. H. New Photoheterolysis Precursors to Study Oxenium Ions: Combining Experiment and Theory. *Org. Biomol. Chem.* **2017**, *15*, 2666−2671.

(17) Dimroth, K.; Umbach, W.; Thomas, H. Stabile Phenoxy-Kationen aus Arylierten Phenolen. *Chem. Ber.* **1967**, *100*, 132−141.

(18) Abramovitch, R. A.; Alvernhe, G.; Bartnik, R.; Dassanayake, N. L.; Inbasekaran, M. N.; Kato, S. Aryloxenium Ions. Generation from N-(Aryloxy)pyridinium Tetrafluoroborates and Reaction with Anisole and Benzonitrile. *J. Am. Chem. Soc.* **1981**, *103*, 4558−4565.

(19) Abramovitch, R. A.; Bartnik, R.; Cooper, M.; Dassanayake, N. L.; Hwang, H. Y.; Inbasekaran, M. N.; Rusek, G. Intramolecular Cyclization of Aryloxenium Ions. Carbon-oxygen-carbon and Carbon-carbon Bond Formation. A Novel *ortho< span=""≫< span=""≫* Effect. *J. Org. Chem.* **1982**, *47*, 4817−4818.

(20) Chakraborty, M.; Brzozowski, C. F.; Novak, M. Reversible Formation of Aryloxenium Ions from the Corresponding Quinols under Acidic Conditions. *J. Phys. Org. Chem.* **2012**, *25*, 1236−1242.

(21) Owen, B. C.; Gao, J.; Borton, D. J., Ii; Amundson, L. M.; Archibold, E. F.; Tan, X.; Azyat, K.; Tykwinski, R.; Gray, M.; Kenttämaa, H. I. Carbon Disulfide Reagent Allows the Characterization of Nonpolar Analytes by Atmospheric Pressure Chemical Ionization Mass Spectrometry. *Rapid Commun. Mass Spectrom.* **2011**, *25*, 1924−1928.

(22) Habicht, S. C.; Vinueza, N. R.; Archibold, E. F.; Duan, P.; Kenttämaa, H. I. Identification of the Carboxylic Acid Functionality by Using Electrospray Ionization and Ion−Molecule Reactions in a

Modified Linear Quadrupole Ion Trap Mass Spectrometer. *Anal. Chem.* **2008**, *80*, 3416−3421.
(23) Manheim, J. M.; Milton, J. R.; Zhang, Y.; Kenttämaa, H. I. Fragmentation of Saturated Hydrocarbons upon Atmospheric Pressure Chemical Ionization Is Caused by Proton-Transfer Reactions. *Anal. Chem.* **2020**, *92*, 8883−8892.
(24) Max, J. P.; Ma, X.; Kotha, R. R.; Ding, D.; Milton, J.; Nash, J. J.; Kenttämaa, H. I. Reactivity of Organic *σ,σ,σ,σ,σ*-Pentaradicals. *Int. J. Mass Spectrom.* **2019**, *435*, 280−290.
(25) Heidbrink, J. L.; Thoen, K. K.; Kenttämaa, H. I. Polar Effects on Iodine Atom Abstraction by Charged Phenyl Radicals. *J. Org. Chem.* **2000**, *65*, 645−651.
(26) Su, T.; Chesnavich, W. J. Parametrization of the Ion−polar Molecule Collision Rate Constant by Trajectory Calculations. *J. Chem. Phys.* **1982**, *76*, 5183−5185.
(27) Milton, J. R.; Jankiewicz, B. J.; Max, J.; Vinueza, N. R.; Kirkpatrick, L. M.; Campbell, K.; Gallardo, V. A.; Reece, J. N.; Kenttämaa, H. I. A Study on the Gas-phase Reactivity of Charged Pyridynes. *J. Org. Chem.* **2021**, *86*, 9979−9993.
(28) Gallardo, V. A.; Jankiewicz, B. J.; Vinueza, N. R.; Nash, J. J.; Kenttämaa, H. I. A Reactivity Study on a 1,2,3,5-Tetradehydrobenzene: the 2,4,6-Tridehydropyridine Radical Cation. *J. Am. Chem. Soc.* **2012**, *134*, 1926−1929.
(29) Dunning, T. H. Gaussian Basis Sets for Use in Correlated Molecular Calculations. I. The Atoms Boron through Neon and Hydrogen. *J. Chem. Phys.* **1989**, *90*, 1007−1023.
(30) Boos, B. O.; Taylor, P. R.; Siegbahn, P. R. A Complete Active Space SCF Method (CASSCF) Using a Density Matrix Formulated Super-CI Approach. *Chem. Phys.* **1980**, *48*, 157−173.
(31) Andersson, K.; Malmqvist, P.-Å.; Roos, B. O.; Sadlej, A. J.; Wolinski, K. Second-order Perturbation Theory With CASSCF Reference Function. *J. Phys. Chem.* **1990**, *94*, 5483−5488.
(32) Andersson, K. Different Formst of the Zeroth-Order Hamiltonian in Second-Order Perturbation Theory With a Complete Active Space Self-Consistent Field Reference Function. *Theor. Chim. Acta* **1995**, *91*, 31−46.
(33) Andersson, K.; Roos, B. O. Multiconfigurational Second-Order Perturbation Theory: A Test of Geometries and Energies. *Int. J. Quantum Chem.* **1993**, *45*, 591−607.
(34) Aquilante, F.; Autschbach, J.; Carlson, R. K.; Chibotaru, L. F.; Delcey, M. G.; De Vico, L.; Fdez. Galván, I.; Ferré, N.; Frutos, L. M.; Gagliardi, L.; Garavelli, M.; Giussani, A.; Hoyer, C. E.; Li Manni, G.; Lischka, H.; Ma, D.; Malmqvist, P. Å.; Müller, T.; Nenov, A.; Olivucci, M.; Pedersen, T. B.; Peng, D.; Plasser, F.; Pritchard, B.; Reiher, M.; Rivalta, I.; Schapiro, I.; Segarra-Martí, J.; Stenrup, M.; Truhlar, D. G.; Ungur, L.; Valentini, A.; Vancoillie, S.; Veryazov, V.; Vysotskiy, V. P.; Weingart, O.; Zapata, F.; Lindh, R. MOLCAS 8: New Capabilities for Multiconfigurational Quantum Chemical Calculations across the Periodic Table. *J. Comput. Chem.* **2016**, *37*, 506−541.
(35) *Gaussian 16*, Revision B.01, Frisch, M. J.; Trucks, G. W.; Schlegel, H. B.; Scuseria, G. E.; Robb, M. A.; Cheeseman, J. R.; Scalmani, G.; Barone, V.; Petersson, G. A.; Nakatsuji, H.; Li, X.; Caricato, M.; Marenich, A. V.; Bloino, J.; Janesko, B. G.; Gomperts, R.; Mennucci, B.; Hratchian, H. P.; Ortiz, J. V.; Izmaylov, A. F.; Sonnenberg, J. L.; Williams-Young, D.; Ding, F.; Lipparini, F.; Egidi, F.; Goings, J.; Peng, B.; Petrone, A.; Henderson, T.; Ranasinghe, D.; Zakrzewski, V. G.; Gao, J.; Rega, N.; Zheng, G.; Liang, W.; Hada, M.; Ehara, M.; Toyota, K.; Fukuda, R.; Hasegawa, J.; Ishida, M.; Nakajima, T.; Honda, Y.; Kitao, O.; Nakai, H.; Vreven, T.; Throssell, K.; Montgomery, Jr., J. A.; Peralta, J. E.; Ogliaro, F.; Bearpark, M. J.; Heyd, J. J.; Brothers, E. N.; Kudin, K. N.; Staroverov, V. N.; Keith, T. A.; Kobayashi, R.; Normand, J.; Raghavachari, K.; Rendell, A. P.; Burant, J. C.; Iyengar, S. S.; Tomasi, J.; Cossi, M.; Millam, J. M.; Klene, M.; Adamo, C.; Cammi, R.; Ochterski, J. W.; Martin, R. L.; Morokuma, K.; Farkas, O.; Foresman, J. B.; Fox, D. J. Gaussian, Inc., Wallingford CT, 2016.
(36) Breneman, C. M.; Wiberg, K. B. Determining Atom-centered Monopoles from Molecular Electrostatic Potentials − The Need for High Sampling Density in Formamide Conformational-analysis. *J. Comput. Chem.* **1990**, *11*, 361−373.
(37) The dissipation of internal energy through IR emission by ions trapped in an ion trap can occasionally be fast compared to the timescale of the experiment. For more information on studies of IR emission rates by trapped ions, see: (a) Dunbar, R. Infrared Radiative Cooling of Gas-Phase Ions. *Mass Spectrom. Rev.* **1992**, *11*, 309−339. (b) Nelson, E. D.; Artau, A.; Price, J. M.; Tichy, S. E.; Jing, L.; Kenttämaa, H. I. *meta*-Benzyne Reacts as an Electrophile. *J. Phys. Chem. A* **2001**, *105*, 10155−10168.
(38) Zhao, Y.; Truhlar, D. G. The M06 Suite of Density Functionals for Main Group Thermochemistry, Thermochemical Kinetics, Noncova-lent Interactions, Excited States, and Transition Elements: Two New Functionals and Systematic Testing of Four M06-class Functionals and 12 Other Functionals. *Theor. Chem. Acc.* **2008**, *120*, 215−241.
(39) (a) Clark, T.; Chandrasekhar, J.; Spitznagel, G. W.; Schleyer, P. V. R. Efficient Diffuse Function-augmented Basis Sets for Anion Calculations. III. The 3-21+G Basis Set for First-row Elements, Li-F. *J. Comput. Chem.* **1983**, *4*, 294−301. (b) Krishnan, R.; Binkley, J. S.; Seeger, R.; Pople, J. A. Self-consistent Molecular Orbital Methods. XX. A Basis Set for Correlated Wave Functions. *J. Chem. Phys.* **1980**, *72*, 650−654.
(40) Ma, X.; Jin, C.; Wang, D.; Nash, J. J.; Kenttämaa, H. I. Relative Reactivities of Three Isomeric Aromatic Biradicals with a 1,4-Biradical Topology Are Controlled by Polar Effects. *Chem.—Eur. J.* **2019**, *25*, 6355−6361.
(41) Ma, X.; Feng, E.; Jiang, H.; Boulos, V.; Gao, J.; Nash, N. N.; Kenttämaa, H. I. Protonated Ground-state Singlet *meta*-Pyridynes React from an Excited Triplet State. *J. Org. Chem.* **2021**, *86*, 3249−3260.
(42) (a) Hunter, E. P. L.; Lias, S. G. Proton Affinity Evaluation. In *NIST Chemistry WebBook, NIST Standard Reference Database Number 69*; Linstrom, P. J., Mallard, W. G., Eds.; National Institute of Standards and Technology: Gaithersburg, MD. (b) Leeck, D. T.; Kenttämaa, H. I. The Heat of Formation of the Radical Cation of Dimethyl Disulfide. *Org. Mass Spectrom.* **1994**, *29*, 106−107.

https://doi.org/10.1021/acs.joc.3c02895
J. Org. Chem. 2024, 89, 5458−5468